

Anodic catalysts for polymer electrolyte fuel cells: the catalytic activity of Pt/C, Ru/C and Pt-Ru/C in oxidation of CO by O₂

Cecilia Bracchini^a, Valerio Indovina^{a,*}, Sergio De Rossi^a, Leonardo Giorgi^b

^a Centro di Studio 'SACSO' CNR c/o Dipartimento di Chimica, Università La Sapienza, P.le A. Moro 5, 00185 Roma, Italy

^b ENEA CR-Casaccia, via Anguillarese 301, 00060 Roma, Italy

Abstract

The catalytic activity for oxidation of CO by O₂ was investigated on commercial Pt/C, Pt-Ru/C (Pt/Ru atomic ratio = 20, 3, 1, 1/3) and Ru/C. All samples contained 20 wt.% metal. Assuming equal surface and bulk composition, the number of surface Pt and Ru atoms was calculated from the average size of the supported metal particle as determined by TEM. On Pt-Ru/C alloys, the turnover frequency per Ru atom, $N_{\text{Ru}}/\text{molecules s}^{-1} \text{ Ru-atom}^{-1}$, was independent of chemical composition. This finding suggests that the active site in these alloys is Ru. In the temperature range 300–400 K, the turnover frequency per active metal atom was 50–300 times higher on Pt-Ru/C than on Pt/C. The turnover frequency was 400 times higher on Ru/C than on Pt/C at 313 K and 90 times higher at 353 K. Addition of water vapor to the reactant mixture left the catalytic activity of Ru/C unchanged but slightly increased the activity of Pt/C. On both catalysts the activation energy and reaction orders were nearly the same as in dry atmosphere. Conversely, the addition of water markedly decreased the activation energy for Pt-Ru(1 : 1)/C alloy (from 19 to 11 kcal mol⁻¹). These findings suggest that fuel cells equipped with Pt-Ru/C anodes perform better than cells with Pt/C anodes. They do so because Ru effectively oxidizes the carbon monoxide present as an impurity in the H₂-reformed fuel. ©2000 Elsevier Science B.V. All rights reserved.

1. Introduction

Because the traditional heat engine is responsible for noxious emissions of CO, NO_x and hydrocarbons, environmental concern has emphasized the need to develop an efficient technological alternative that will increase the efficiency of fuel-energy conversion thus minimizing air pollution and the greenhouse effect. Fuel cells are electrochemical devices which convert the energy of the gas phase reaction between a fuel and an oxidant directly and continuously into electrical energy with high power density, high energy conversion efficiency and very low environmental intrusion. Fuel

cells and their applications have been exhaustively described by Bockris and Srinivasan [1], Appleby and Foulkes [2] and Kordesch et al. [3].

Electrocatalytic combustion occurring in polymer electrolyte fuel cells (PEFCs) is a clean technology with virtually zero emissions therefore representing a primary polluting prevention system [4]. In a typical PEFC (Pt-based gas diffusion electrodes and acidic polymer electrolyte), humidified H₂ and O₂ react at the anode (H₂ electrooxidation) and cathode (O₂ electroreduction), at about 353 K. Hence, the overall cell reaction produces nothing other than electricity, water and heat.

In addition to zero harmful emissions, PEFCs have other advantages. They possess higher practical efficiency than thermal engines. They also provide a more effective energy-storage system, higher power

* Corresponding author. Tel.: +39-06-4991-3381;
fax: +39-06-490324
E-mail address: indovina@axrma.uniroma1.it (V. Indovina)

density, much longer operating life and better weight and volume features than conventional batteries (Pb-acid, Ni-Cd, Ni-H). In addition, compared with alkaline fuel cells and phosphoric acid fuel cells, PEFCs have a higher power density, an absence of liquid electrolyte and a lower operating temperature, thus minimizing corrosion problems.

At present, PEFC-powered electrical prototypes run on pure hydrogen. The use of this fuel for a mass market application is limited by purification costs, lack of proper refuel infrastructures, large storage volume and security problems. Current attention is, therefore, focused on H_2 rich gas produced by reforming of methanol on board the vehicle. A typical reformate mixture consists roughly of hydrogen (75%), carbon dioxide (24%) and carbon monoxide (1%). Carbon monoxide drastically affects the way PEFCs perform. When the reformer is paired with a water shift reactor followed by an oxidation reactor selective for CO, carbon monoxide can be abated to 10 ppm [5]. At the operational temperature, carbon monoxide even at ppm levels poisons Pt catalysts [6–8]. One way of overcoming the problem is to use Pt-Ru electrodes [9–13]. To explain the positive effect of Ru, Gasteiger et al. [9–11], Ianniello et al. [12] and Oetjen et al. [13] proposed that water activation causes an oxygen-containing species (Ru-OH) to form on Ru, thereby favoring effective removal of carbon monoxide from an adjacent Pt site (oxidative disposal of the poisoning CO). At variance, Cooper et al. [14] proposed that the presence of ruthenium prevents the formation of stable platinum carbonyls.

Within this framework, we investigated the $CO + O_2$ reaction on Pt/C, Pt-Ru/C alloys (Pt/Ru atomic ratio equal to 20, 3, 1, 1/3) and Ru/C. All samples contained 20 wt.% metal (Pt, Pt + Ru or Ru). Samples were characterized by means of X-ray diffraction (XRD), energy dispersive spectroscopy (EDS) and transmission electron microscopy (TEM). On the same catalysts, electrochemical experiments (electrochemical impedance spectroscopy and cyclic voltammetry) are in progress. Preliminary results suggest that as anode catalysts for PEFCs in the presence of CO, Pt-Ru/C perform better than Pt/C [15]. Catalytic results are reported here in full. Characterization data relevant to the discussion of the catalytic activity will be given, whereas details on characterization of the catalysts will be reported elsewhere [15].

2. Experimental

2.1. Catalysts and characterization techniques

Commercial powder catalysts Pt, Pt-Ru (Pt/Ru = 20, 3, 1, 1/3 atomic ratio) and Ru, all supported on carbon black (Vulcan XC72 Cabot Co.) were purchased from E-TEK Inc. (Natick, MA). All samples contained 20 wt.% metal. The nominal composition was checked by microchemical analysis (EDS).

X-ray diffraction spectra were recorded with a Philips powder diffractometer (Model PW 1710) using a $Cu\ K\alpha$ source. The 2θ -angular region between 20 and 140° was investigated with a scan speed of $0.025^\circ\ s^{-1}$.

Transmission electron microscopy data were acquired with a Jeol 4000FX analytical electron microscope. Specimens for TEM were prepared by suspending the catalyst powder in isopropyl alcohol. A drop of suspension was then applied onto copper grids.

2.2. Catalytic experiments

The catalytic activity was measured in a conventional flow apparatus at atmospheric pressure. The apparatus included a feeding section where the three-gas stream (He, 2% O_2 in He, and 3% CO in He, high purity purchased from Rivoira) was regulated by means of independent mass flow controller meters (MKS mod. 259, driven by a four-channel unit MKS mod. 247 c) and mixed in a glass ampoule before entering into the reactor. The reactor was made of silica with an internal sintered frit of about 12 mm diameter supporting the powdered catalysts. The reactor was vertically positioned in an electrical heater, with a thermocouple touching the external wall of the reactor at the middle of the catalyst bed. A commercial device was used to regulate temperature. A reactor bypass was provided by a four-way valve. Reactants and products were analyzed by gas chromatography (Varian mod. 6000 gas chromatograph, equipped with an Alltech CTR 1 column kept at 308 K). A thermal conductivity detector (TCD) was used for detecting all compounds. Peak areas were evaluated by electronic integration.

A fresh portion of catalyst (0.2–0.5 g) was purged in flowing He at RT for 20 min, heated from RT to 623 K in a flow of 3% CO in He mixture for 0.5 h

Table 1
Reaction order, activation energy and turnover frequency for the CO + O₂ reaction

Catalyst	d^a (nm)	Me S^b	Reaction order		E_a (kcal mol $^{-1}$)	$N_{\text{Pt+Ru}}^c$	N_{Pt}^c	N_{Ru}^c	N_{Ru}^c
			O ₂	CO		at 353 K			at 313 K
Pt/C	2.6	2.7×10^{20}	0.8	−0.5	17	7.5×10^{-6}	7.5×10^{-6}	–	
Pt-Ru(20 : 1)/C	2.6	2.8×10^{20}	0.9	−0.5	16	2.3×10^{-5}	2.4×10^{-5}	4.8×10^{-4}	
Pt-Ru(3 : 1)/C	1.9	4.2×10^{20}	0.7	−0.5	18	1.6×10^{-4}	2.2×10^{-4}	6.5×10^{-4}	
Pt-Ru(1 : 1)/C	2.1	4.4×10^{20}	0.8	−0.6	19	3.0×10^{-4}	6.1×10^{-4}	6.1×10^{-4}	2.4×10^{-5}
Pt-Ru(1 : 3)/C	2.1	5.2×10^{20}	0.6	−0.5	19	1.5×10^{-3}	6.1×10^{-3}	2.0×10^{-3}	
Ru/C	2.8	5.7×10^{20}	0.3	−0.3	8	5.6×10^{-4}	–	5.6×10^{-4}	1.4×10^{-4}

^a Average size of the metal particle from TEM.

^b Surface metal atoms (Pt + Ru) gram^{−1} of catalyst, calculated assuming spherical particles and 12.5 Me-atoms nm^{−2} for Pt/C and Pt-Ru/C, and 16.3 Me-atoms nm^{−2} for Ru/C sample [16].

^c Turnover frequencies (*N*/molecules s^{−1} atom^{−1}) *N*_{Pt}, *N*_{Ru}, *N*_{Pt+Ru} normalized with respect to Pt, Ru or Pt + Ru atoms, in that order.

and then held at 623 K for 2 h. After purging with He at 623 K for 1 h, the reactor was bypassed and the temperature adjusted to the desired value. Catalysis experiments were run using stoichiometric mixtures of CO (0.4%) and O₂ (0.2%) with He as balance. In some experiments, the gas stream was humidified by bubbling it into water at 273 K (H₂O 6000 ppm). After stabilization of the reactants, the four-way valve was switched and the reaction mixture was allowed to flow onto the catalyst. The reaction temperature or mixture composition was changed without intermediate activation treatment. The total flow rate, *F*_t, was generally maintained at 50 ml(STP) min^{−1}. In the range 20–70 ml(STP) min^{−1}, rates were independent of total flow. The reaction rate, *r*, calculated from the CO₂ produced or CO consumed, was expressed as molecules of CO converted to CO₂ s^{−1} g^{−1} of catalyst. Reaction rates (*r*/CO₂ molecules s^{−1} g^{−1}) were evaluated from experiments yielding conversion of less than 50%.

3. Results and discussion

3.1. XRD analysis

Pt/C catalysts exhibited the diffraction peaks of the Pt fcc structure (JCPDS 4-802), Ru/C catalysts those of the Ru hcp structure (JCPDS 6-663). Pt-Ru/C showed only Pt diffraction peaks. These peaks shifted to higher 2θ values as the Ru content increased, suggesting a continuous decrease in the cell parameter. Irrespective of the chemical composition, the aver-

age size of the metal particle, determined from line broadening, was 2.0 ± 0.4 nm.

3.2. Transmission electron microscopy analysis

The bright field images of the catalysts indicated that the metal particles on the carbon support had a uniform distribution. The particle-size distribution was determined from the analysis of different regions of the same catalyst. The average size of the metal particle decreased passing from Pt/C and Ru/C to the alloys (Table 1). The estimated error on the metal particle mean size was ±0.2 nm. The standard deviation, σ, of the particle size distribution was 0.6–0.9 nm.

3.3. Catalytic activity for the CO + O₂ reaction

Comparison of steady-state activity for the CO + O₂ reaction of Pt/C, and Pt-Ru/C alloys (Pt/Ru atomic ratio = 20, 3, 1, 1/3) showed that Pt-Ru/C catalysts were more active than Pt/C catalysts: the higher the Ru content the greater their activity (Fig. 1). On alloys, the reaction orders (O₂, 0.7 and CO, −0.5, Table 1) and the activation energy (16–19 kcal mol^{−1}, Table 1) were nearly independent of Ru content. These data suggest that all the Pt-Ru/C catalysts operate via the same mechanism and that the active site is Ru. From the average size of the metal particle as determined from TEM, assuming the surface composition of the alloy particles equaled the bulk composition, we calculated the concentration of the surface metal atoms (Pt, Pt + Ru or Ru). From these values, we calculated the

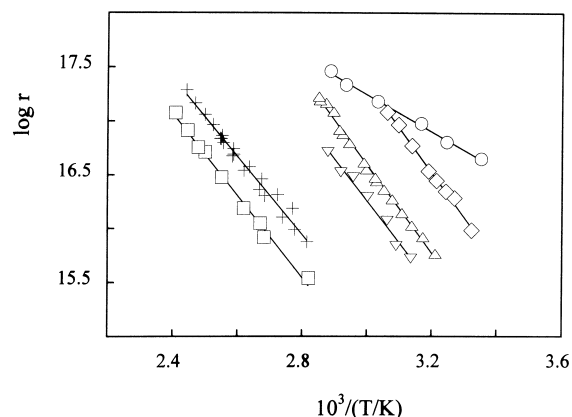


Fig. 1. The dependence of catalytic activity on the ruthenium content. Arrhenius plot ($\log r$ versus $1/T \times 10^3$; r/CO_2 molecules $\text{s}^{-1} \text{g}^{-1}$). Catalysts: \square Pt/C, \triangle Pt-Ru(1:1)/C, \circ Ru/C, \diamond Pt-Ru(1:3)/C, ∇ Pt-Ru(3:1)/C, + Pt-Ru(20:1)/C.

turnover frequency values as CO_2 molecules produced per second and per (i) surface Pt + Ru atom ($N_{\text{Pt+Ru}}$, Column 7, Table 1), (ii) surface Pt atom (N_{Pt} , Column 8, Table 1), and (iii) surface Ru atom (N_{Ru} , Columns 9 and 10, Table 1). In particular, surface metal atoms $(\text{Pt} + \text{Ru}) \text{g}^{-1}$ of catalyst, Me_S , were calculated assuming spherical particles and $12.5 \text{ Me-atoms nm}^{-2}$ for Pt/C and Pt-Ru/C, and $16.3 \text{ Me-atoms nm}^{-2}$ for Ru/C sample [16]. Turnover frequency was, thus, calculated as $N_{\text{Me}} = r/\text{Me}_\text{S} X_{\text{Me}}$, where X_{Me} is the molar fraction of the metal (Pt or Ru, or both).

On Pt-Ru/C alloys, when the Pt/Ru ratio changed from 20 to 1, N_{Ru} was independent of the chemical composition but on the alloy with the highest Ru content (Pt/Ru = 1/3) N_{Ru} increased by a factor of about four. By contrast, on the same catalysts, N_{Pt} and $N_{\text{Pt+Ru}}$ increased by a factor of about 100. Our observation that N_{Ru} changed much less than N_{Pt} and $N_{\text{Pt+Ru}}$, again argues in favor of Ru as the active site for the $\text{CO} + \text{O}_2$ reaction in Pt-Ru/C catalysts.

Having assessed that Ru is the active site in the Pt-Ru/C catalysts, we next compared the activity of Pt-Ru/C with that of Pt/C and Ru/C catalysts. Because Pt/C and Pt-Ru/C catalysts exhibit similar reaction orders in O_2 and CO and similar activation energies, their activities can be compared at any temperature in the range 294–417 K. The comparison shows that the turnover frequency per active metal atom was 50–300 times higher on Pt-Ru/C than on Pt/C catalysts. Conversely, because Ru/C and Pt-Ru/C exhibit

rather dissimilar activation energy and reaction orders, their activity must be compared at two temperatures (313 and 353 K). At 313 K the turnover frequency was 400 times higher on Ru/C than on Pt/C, and at 353 K 90 times higher.

The observed activity pattern, namely $\text{Ru/C} \gg \text{Pt/C}$, contrasts with the pattern reported for pure Ru and Pt single crystals ($\text{Pt} \gg \text{Ru}$) [17] and for Pt and Ru supported on silica ($\text{Pt/SiO}_2 > \text{Ru/SiO}_2$) [18], but it is in agreement with the electrochemical behavior in the electrooxidation of carbon monoxide ($\text{Ru} \approx \text{Pt-Ru} \gg \text{Pt}$) [9].

The effect of adding water to the $\text{CO} + \text{O}_2$ mixture was investigated on Pt/C, Ru/C and Pt-Ru(1:1)/C (Fig. 2; Table 2). In the absence of O_2 , no CO_2 was produced showing that the $\text{CO} + \text{H}_2\text{O}$ reaction did not occur. In the presence of water vapor, the catalytic activity of Ru/C for $\text{CO} + \text{O}_2$ remained nearly unchanged, whereas that of Pt/C increased slightly. On both catalysts, activation energy and reaction orders

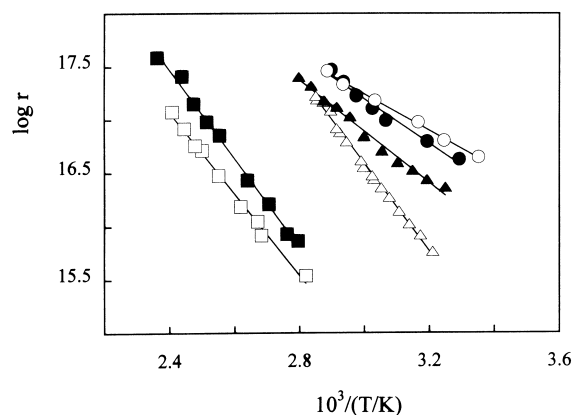


Fig. 2. The catalytic activity of \square \blacksquare Pt/C, \circ \bullet Ru/C, \triangle \blacktriangle Pt-Ru(1:1)/C for the $\text{CO} + \text{O}_2$ reaction in the absence of water vapor (open symbols) and in the presence of water vapor (solid symbols). Arrhenius plot ($\log r$ versus $1/T \times 10^3$; r/CO_2 molecules $\text{s}^{-1} \text{g}^{-1}$).

Table 2

Reaction order and activation energy for the $\text{CO} + \text{O}_2$ reaction in the presence of water

Catalyst	Reaction order in O_2	Reaction order in CO	E_a (kcal mol^{-1})
Pt/C	0.6	−0.5	19
Pt-Ru(1:1)/C	0.6	−0.6	11
Ru/C	0.3	−0.3	10

remained nearly unchanged. On the addition of water, however, the activation energy of the Pt-Ru(1:1)/C alloy markedly decreased (from 19 to 11 kcal mol⁻¹).

4. Conclusions

As catalysts for the oxidation of CO with O₂, Pt-Ru/C alloys perform better than pure Pt/C, thus paralleling their electrochemical behavior [9].

Fuel cells equipped with Pt-Ru/C anodes perform better than cells with Pt/C anodes because Ru facilitates oxidation of the carbon monoxide present as an impurity in the H₂-reformed fuel. At the fuel cell operating-temperature (353 K), the addition of water vapor to the reactant mixture leaves the catalytic performance of Pt/C and Pt-Ru/C virtually unchanged.

References

- [1] J.O' M. Bockris, S. Srinivasan, in: *Fuel Cells: Their Electrochemistry*, McGraw-Hill, New York, 1969
- [2] A.J. Appleby, F.R. Foulkes, in: *Fuel Cell Handbook*, Van Nostrand Reinhold, New York, 1989
- [3] K. Kordesch, G. Simader, in: *Fuel Cells and Their Applications*, VCH, Weinheim, Germany, 1996
- [4] J.A. Cusumano, *Appl. Catal., A: General* 113 (1994) 181.
- [5] S.J.C. Cleghorn, X. Ren, T.E. Springer, M.S. Wilson, C. Zawodzinski, T.A. Zawodzinski, S. Gottesfeld, *Int. J. Hydrogen Energy* 22(12) (1997) 1137.
- [6] P. Stonehart, G. Kohlmayr, *Electrochim. Acta* 17 (1972) 369.
- [7] W. Vogel, J. Lundquist, P. Ross, P. Stonehart, *Electrochim. Acta* 20 (1975) 79.
- [8] S. Gottesfeld, J. Paddorf, *J. Electrochem. Soc.* 135 (1988) 2651.
- [9] H.A. Gasteiger, N.M. Markovic, P.N. Ross Jr., E.J. Cairns, *J. Phys. Chem.* 98 (1994) 617.
- [10] H.A. Gasteiger, N.M. Markovic, P.N. Ross Jr., *J. Phys. Chem.* 99 (1995) 8290.
- [11] H.A. Gasteiger, N.M. Markovic, P.N. Ross Jr., *J. Phys. Chem.* 99 (1995) 16757.
- [12] R. Ianniello, V.M. Schmidt, U. Stimming, J. Stumper, A. Wallau, *Electrochimica Acta* 39(11/12) (1994) 1863.
- [13] H.F. Oetjen, V.M. Schmidt, U. Stimming, F. Trila, *J. Electrochem. Soc.* 143 (1996) 3838.
- [14] S.J. Cooper, A.G. Gunner, G. Hoogers, D. Thompsett, in: *Proceedings of a Conference on New Materials for Fuel Cell and Modern Battery System II*, 6–10 July 1997, Montreal, Que., Canada
- [15] C. Bracchini et al., in press
- [16] J.R. Anderson, in: *Structure of Metallic Catalysts*, Academic Press, 1975, p. 296
- [17] T. Engel, G. Ertl, *Adv. Catal.* 28 (1979) 1.
- [18] K.F. Blurton, J.R. Stetter, *J. Catal.* 46 (1977) 230.